geosciences

MDPI

Article

Geomorphology and Late Pleistocene–Holocene Sedimentary Processes of the Eastern Gulf of Finland

Daria Ryabchuk [1,2,*], Alexander Sergeev [1], Alexander Krek [3], Maria Kapustina [3], Elena Tkacheva [3,4], Vladimir Zhamoida [1,2], Leonid Budanov [1,5], Alexandr Moskovtsev [1] and Aleksandr Danchenkov [3,4]

1 A.P. Karpinsky Russian Geological Research Institute (VSEGEI), 74, Sredny prospect, 199106 Saint Petersburg, Russia; sergeevau@yandex.ru (A.S.); Vladimir_Zhamoida@vsegei.ru (V.Z.); leon_likes@mail.ru (L.B.); aleks_moskovtsev@vsegei.ru (A.M.)
2 Institute of Earth Science, St. Petersburg State University, 7–9 Universitetskaya Embankment, 199034 Saint Petersburg, Russia
3 Shirshov Institute of Oceanology, Russian Academy of Sciences, 36, Nahimovskiy prospekt, 117997 Moscow, Russia; av_krek_ne@mail.ru (A.K.); Kapustina.mariya@ya.ru (M.K.); elenatkacheva_kg@mail.ru (E.T.); aldanchenkov@mail.ru (A.D.)
4 Institute of Environmental Management, Urban Development and Spatial Planning, I. Kant Baltic Federal University, 14, Nevskogo Alexandre street, 236016 Kaliningrad, Russia
5 Faculty of Geological Prospecting, Saint-Petersburg Mining University, 21 Line, 2, 199106 Saint Petersburg, Russia
* Correspondence: Daria_Ryabchuk@mail.ru; Tel.: +7-921-789-3367

Received: 8 December 2017; Accepted: 14 March 2018; Published: 18 March 2018

Abstract: In 2017, a detailed study of the Eastern Gulf of Finland (the Baltic Sea) seafloor was performed to identify and map submerged glacial and postglacial geomorphologic features and collect data pertinent to the understanding of sedimentation in postglacial basins. Two key areas within the Gulf were investigate using a multibeam echosounder, SeaBat 8111 and an EdgeTech 3300-HM acoustic sub-bottom profiling system. High-resolution multibeam bathymetric data (3-m resolution) were used to calculate aspect, slope, terrain ruggedness and bathymetric position index using ArcGIS Spatial Analyst and the Benthic Terrain Modeler toolbox. These data and resultant thematic maps revealed, for the first time, such features as streamlined till ridges, end-moraine ridges, and De Geer moraines that are being used for the reconstruction of the deglaciation in the Eastern Gulf of Finland. This deglaciation occurred between 13.8 and 13.3 ka BP (Pandivere–Neva stage) and 12.25 ka BP (Salpausselkä I stage). Interpretations of the seismic-reflection profiles and 3D models showing the surfaces of till, and the identification of the Late Pleistocene sediment and modern bottom relief, indicate deep relative water-level fall in the Early Holocene and, most likely, several water-level fluctuations during this time.

Keywords: geomorphology; submerged glacial bedforms; deglaciation; sedimentation; multibeam; acoustic-seismic profiling

1. Introduction

The Baltic Sea is an ideal natural laboratory [1] for the study of geologically-induced driving forces of different sea bottom and coastal zone processes (e.g., the intensity of sedimentation and erosion processes and areas of their distribution, sediment flows, geochemical processes, benthic landscape development). Understanding these forces is important for the sustainable use of natural resources and environmental protection [2,3]. In addition, some Baltic Sea basins are crucial for the understanding of postglacial geological history and recent sedimentation processes. These basins

are located in subsiding areas within the Southern and Southwestern Baltic Sea [1,4–6] and regions of uplift are located within the Northern Baltic Sea [7]. Several key areas of the Eastern Baltic Sea are very important for modelling historic and present tectonic processes (e.g., Eastern Gulf of Finland and Pärnu Bay), which are characterized by very low (from 0 to +3 mm/year) rates of uplift—a near zero rate of recent sea level change. According to a datum obtained by a Kronshtadt gauge measurement, the rate of sea level rise from 1835 to 2005 was 0.7 mm/year [8]. The combination of tectonic processes, total sea bottom coverage by Quaternary deposits, relatively smooth and shallow relief, and widespread Holocene accretion, both above and below the recent sea level, is useful geological and geomorphological information that can be used to reconstruct palaeoenvironmental changes [9–13].

Between 1986 and 2000, the Eastern Gulf of Finland was mapped by the Russian Research Geological Institute (VSEGEI) [14], resulting in the publication of a State Geological Survey Map (1:200,000 scale). Approximately 8000 km of seismic reflection sub-bottom profiles (SBP) and more than 6000 sampling sites were used in the mapping effort. The SBP lines were oriented mainly parallel to meridians and spaced approximately 2 km apart. Two acoustic sources were synchronously operated, one with a fundamental frequency of 500 Hz (sparker) and another at a frequency of 7.5 kHz (piezoceramic transmitter). More than 6000 sediment samples including 4000 gravity cores were collected and used for SBP data interpretation. In 2009 and 2011, during joint Russian–Finnish field cruises on board the R/V *Aranda* of the Finnish Environment Institute, approximately 800 km of 12-kHz pinger sub-bottom profiles were collected by Meridata Ltd. [15]. Recently, these profiles were digitized and analysed using GIS methods. Assessment of regional deglaciation processes and postglacial sedimentation was undertaken to form 3D models compiled of pre-Quaternary relief, consisting of moraines and Late Pleistocene surfaces, from which the thicknesses of till, glacio-lacustrine, and Holocene sediments were calculated [16].

Despite a relatively high confidence in the geology reported to date for the area of our study, there still remain important unsolved problems, specifically those pertaining to the postglacial geological history including (i) the location of end moraines and glaciofluvial deposits in the Gulf of Finland; (ii) the age of deglaciation and rate of glacial front retreat; and (iii) the number of Holocene sea level fluctuations and the amplitude of relative regressions [13,16]. The best known regional palaeoreconstructions of deglaciation were reported by I. Krasnov (International Map of the Quaternary deposits of Europe, [17], E. Zarrina [18], D. Kvasov [19], A. Raukas [20], D. Subetto [21], and J. Vassiljev [22]. These reconstructions were based on terrestrial investigations where locations of ice-sheet margins within the Gulf of Finland basin are generally shown on maps by dashed lines (inferred) or attributed as unknown [23]. Hypothesized locations of terminal moraines formed during the Pandivere–Neva stage east of Kotlin Island [18] or near the Eastern coast of Narva Bay to Cape Peschany [21] have not been documented as there is no geomorphological or chronological evidence for these glacial forms. The problem regarding Holocene sea level fluctuation, especially the location of regression levels is the subject of much discussion today [9–13].

Recent advances in marine geological methodology and technology using multiple instruments, such as high-resolution geophysical SBP, multibeam echosounder bathymetry and backscatter, and side-scan sonargraphs have provided data that is useful for the 3D geomorphometric visualization of submerged surfaces, which has significantly improved our knowledge of sea bottom relief and geological structure [24–29]. In the Eastern (Russian) part of the Gulf of Finland, the first attempts at using these state-of-the-art geological and geophysical methodologies focused on the study of geological hazards, such as submarine landslides, pockmarks [30,31], and processes associated with Fe–Mn concretion and regeneration, based on exploration [32] undertaken by VSEGEI between 2012 and 2014. The exploration was part of a Russian National project entitled “State Monitoring of Geological Environment of Near-Shore Areas of Russian Baltic, Barents and White Seas” and a Russian–Finnish project entitled “Transboundary Tool for Spatial Planning and Conservation of the Gulf of Finland” (TOPCONs) (a project of the European Neighbourhood and Partnership Instrument

(ENPI) Program) [3]. Unfortunately, the areas covered using high-resolution geophysical equipment in the Eastern Gulf of Finland during these campaigns were limited.

This paper presents the first results of the interpretation of multibeam and SBP data collected during a joint Atlantic Branch of the Institute of Oceanology of Russian Academy of Science (ABIO RAS) and VSEGEI cruise on board R/V Academic Nikolaj Strakhov in the Eastern Gulf of Finland during the summer of 2017. The main goal of this paper is to present new high resolution geophysical data and morphometric analyses from that area of the Gulf of Finland which had previously lacked good data for understanding and mapping the marine geology. A high resolution geophysical survey carried out within two key areas of the Eastern Gulf of Finland imaged, for the first time, submerged glacial and postglacial bottom features and provided new data that can be used to interpret sedimentation within the postglacial basins of the Northeastern Baltic Sea (Figure 1A). The main criteria for choosing the key areas was the possible occurrence of variety in submerged glacial and glaciofluvial landforms and transition zones from relative bathymetric high areas to sediment basins.

Study Area

The Eastern Gulf of Finland is located at the boundary between the Russian Plate and the Southeastern margin of the Baltic crystalline shield. A peneplain surface, now gently sloping south–southeast, was eroded into Paleo–Mesoproterozoic basement prior to the commencement of the Late Vendian–Early Paleozoic terrigenous sedimentation event. Tertiary denudation, including dominant glacial erosion, was instrumental in forming the present bedrock topography, both in the Southern sediment-covered part of the region and in the shield [14].

Quaternary sediment almost completely covers the bottom and coastal areas of the Eastern Gulf of Finland, except locally in Vyborg Bay and on some islands. The Pleistocene geological record locally exhibits till (ground moraines), deposited during the last glaciation, glacio-lacustrine sediments of ice marginal lakes and the Baltic Ice Lake (varved and homogenous clays), and local glaciofluvial sands. The lower part of the Holocene is represented by the Ancylus Lake clays with microlenses of black amorphous Fe–sulphides. The upper part of the sedimentary section was formed during the Littorina and Post-Littorina sea phases of the Baltic Sea's development. These sediments are represented by silty clay mud and sands. Boulders and pebbles form the tops of submarine highs and the upper parts of coastal slopes in the areas of intense submarine erosion. Sands of different grain sizes and geneses (from unsorted relict sands of the Gulf proper to fine-grained, very well sorted wave accretion sands of the near shore zone) are the most widespread type of bottom sediment. Sandy clays and silts are usually connected with areas of non-sedimentation (transitional zones) and weak submarine currents. Clayey mud accumulation occurs within bottom depressions. A unique type of sediment is represented by Fe–Mn concretions [14].

2. Material and Methods

2.1. Broad-Scale Data Analysis

To pinpoint the potential location of submarine end moraine complex data from previous investigations of the Eastern Gulf of Finland, Quaternary deposits, bottom relief, and palaeogeographic development since the last deglaciation were utilized. To obtain new data about regional deglaciation and postglacial development, 3D models of pre-Quaternary relief, moraine and Late Pleistocene surfaces were compiled; the thicknesses of the till, glacio-lacustrine and Holocene sediments were calculated based on interpretations of the seismic reflection profiles collected between 1986 and 2000. A broad scale bathymetric model of the Eastern Gulf of Finland bottom was analysed using traditional GIS instruments, which allowed us to localize submarine landforms, which were further interpreted using all available geological and geophysical information (Figure 1). The results of these interpretations were used to select key areas for field multibeam and acoustic-seismic surveys.

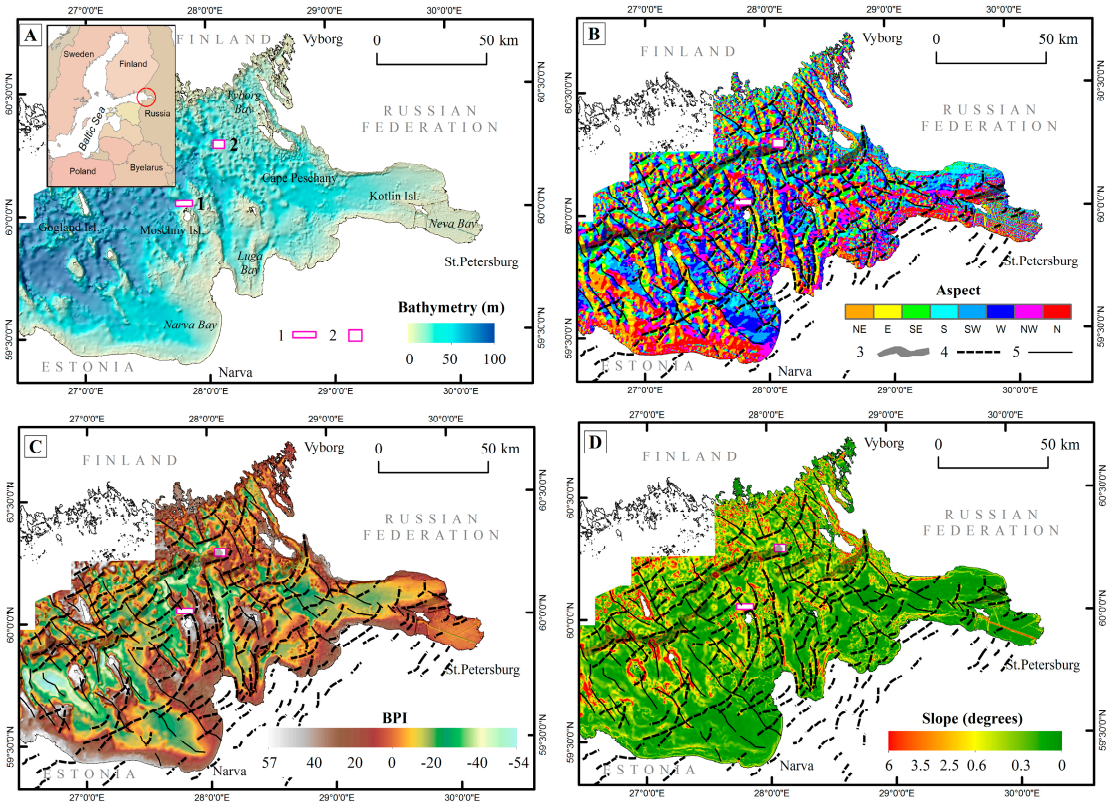

Figure 1. Broad scale models of the Eastern Gulf of Finland bottom relief. (**A**) bathymetry. Bottom relief is relatively shallow. Depths gradually rise from the east (2–5 m in Neva Bay) to west (70–80 m around Gogland Island); (**B**) bathymetry aspect map overlayed upon the till surface. The results of analysis facilitated the interpretation of the most probable location of recessional moraines and streamlined moraine features; (**C**) Bathymetric Position Index (BPI); (**D**) slope. Note: most parts of the Eastern Gulf of Finland bottom relief are very smooth (with a slope angle of less than 1°). Maximum slope angles (up to 6°) are observed in the Northwestern part of the study area (blocks 1, 2, key areas selected for multibeam surveys in 2017; 1 = Moschny Island area; 2 = Vyborg Bay area in (**A**); 3 = predicted end-moraine areas according to sub-bottom profile (SBP) data (1986–2000) interpretations (see **B** for symbol); 4 = assumed till relief features parallel to ice-sheet margin (see **B** for symbol); 5 = assumed streamlined till relief features (see **B** for symbol) [16]. The colour ramp has been selected to highlight the main features of the terrain.

2.2. Multibeam Echosounding and Acoustic-Seismic Profiling Equipment

During the cruise of the R/V Academic Nikolaj Strakhov (19–25 July 2017) two key areas in the Eastern Gulf of Finland were studied using a multibeam echosounder (MBES) and SBP (Figure 2). In the Vyborg Bay key area, thirty-nine lines of MBES and SBP tracks (total length is 164 km) were run to provide a coverage area of 9 km^2 (Figure 2A). Thirty-three lines of MBES and SBP (total length of 119 km) in the Moschny Island key area covered 6.8 km^2 (Figure 2B).

The R/V Academic Nikolaj Strakhov is equipped with a Teledyne RESON Seabat 8111-E208-3F66 Dry MBES system and an EdgeTech 3300-HM sub-bottom profiler (with Discover Sub-Bottom v3.36). Data collection and primary processing were undertaken using PDS2000 v3.7.0.47 processing software.

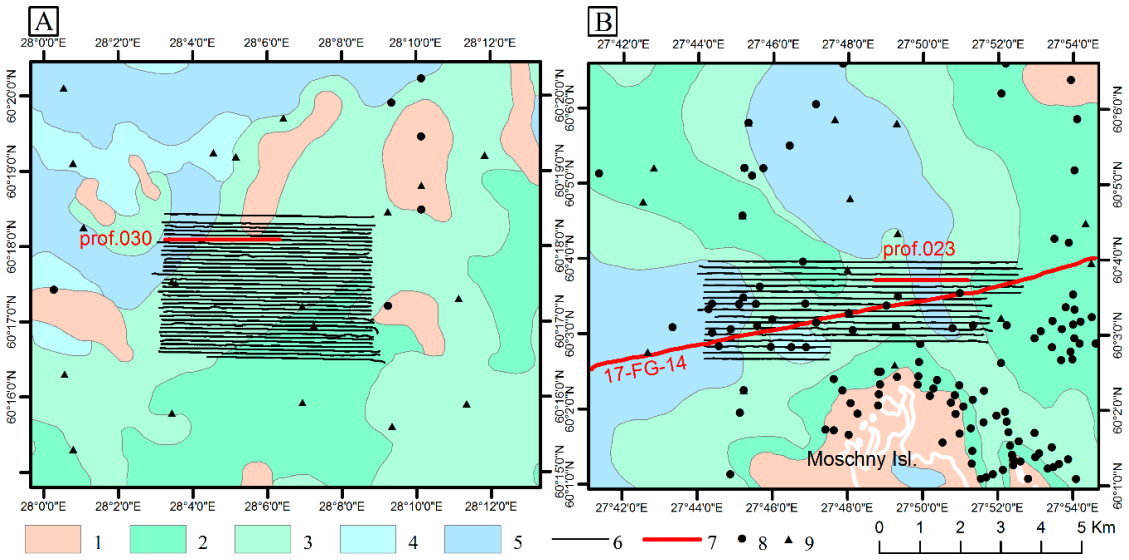

Figure 2. Part of a Quaternary deposits map of key study areas [14] with multibeam echosounder (MBES) and SBP profile tracks (solid black lines) and sampling stations (black dots). (**A**) Vyborg Bay; (**B**) Northern area off Moschny Island. Late Pleistocene sediment shown as (1) till; (2) varved clays; (3) homogenous clays of the Baltic Ice Lake. Holocene sediment shown as (4) Ancylus Lake clays, (5) Littorina—Post-Littorina marine silty-clayey muds. Geophysical data collection lines shown as (6) MBES and SBP (2017); (7) SBP, described in this article. Sample locations: (8) grab-corers and box-corers, (1984–2017); (9) long gravity corers (1984–2000).

The MBES data were collected using an operating frequency of 100 kHz. The area was covered by 101 beams at 1.5° × 1.5°, 150° perpendicular to the direction of travel and 1.5° in the direction of travel. The resolution of each beam, regardless of the distance away from nadir, was 3.7 cm. The EdgeTech 3300-HM fundamental frequency range was 2–10 kHz with a pulse width of 5 to 100 ms at a sampling rate of either 20, 25, 40, or 50 kHz, depending on the pulse of the higher frequency. To calculate depths and positions, data from external GPS and motion sensors fixed to the vessel were used. The position of these sensors and GPS antennas were located at the same reference point, corresponding to the point of the OCTANS sensor arrangement, which was installed at the waterline as close as possible to the x-axis of the vessel. Georeferencing of data received from the sensors was carried was in the WGS-84 coordinate system.

An additional seismic-reflection profile (17-FG-14) was collected in the Moschny Island key area on board the R/V SN 1303 in September 2017 (Figure 2B). The SBP survey was performed using a GEONT-HRP "Spektr-Geophysika" Ltd. (Russian) sparker, operated at a working frequency range of 0.03 to 2 kHz. The vessel continuously recorded positions using the Differential Global Positioning System (DGPS) with ± 5 m accuracy (Furuno GP7000F system in combination with Vector VS330 (Hemisphere GNSS, Scottsdale, AZ, USA).

2.3. Calibration

Before the bathymetric survey, the MBES system was calibrated on a flat seabed and along a slope. The purpose of calibration was to determine the systematic errors in the measured values (depth, coordinates) and to exclude these errors from the good data. The MBES standard calibrations (roll, pitch, yaw) were performed using the PDS2000 automatic program. The corrections received were used during the survey. A Sea&Sun Tech CTD90 multi-parameter probe was used prior to the survey, in the deepest part of the acoustic polygon, to obtain water column velocities which were recorded in the PDS2000 user files.

2.4. Multibeam Bathymetry Data Processing

Three main stages of data processing were designed using the PDS2000 and ArcGIS 10.2 software packages. Subsequent processing and calculation of seafloor attributes led to the construction of geomorphic and substrate maps.

2.4.1. Stage 1. Initial Data Processing Using the Default Software Package, PDS2000

Primary processing of the data was carried out using PDS2000 software. This process consisted of two main steps: (1) data cleaning with filters; and (2) post-processing and manual cleaning. Systematic depth distortions along with edge beam inaccuracies were removed with data filtering. Further manual processing removed non-systematic distortions. After processing, the data were exported in ASCII format (xyz) to a GIS project.

A 10-m cell size was chosen for creating the preliminary bathymetric grid. The grid was used for the visual assessment of systematic errors in the data array (e.g., furrows, scanning lines). If there were no visible artefacts, all of the accepted depths were exported in ASCII (xyz) format for further morphometric analysis.

2.4.2. Stage 2. Data Import into ArcGIS and Generation of the Digital Bathymetric Model (DBM)

Importation of a separate survey was carried out by ArcGIS tool ASCII 3D to Feature Class for converting large data sets into the 3D ASCII XYZ format. The data sets were then coupled into a single sonar point cloud data with extraction of Z-data as an additional text field from the 3D Shp file.

Due to the high density of the initial data sets (1–2 m between the cloud points), the Natural Neighbor method was used to construct the digital terrain model, a method based on Voronoy tessellation for discrete data [33]. A normal digital terrain model constructed using a 3-m-grid (25 m^2), which resulted in striped artefacts associated with the initial reflections (side and central beams).

2.4.3. Stage 3. Reduction of Bathymetric Data Artefacts with the Use of the ArcGIS Software

The reduction of the depth artefacts consisted of two main steps. The first step was noise smoothing on the surface of the digital model using a local linear polynomial approximation (the nearest 15 measurements were used for the approximation). The second step was de-striping the measured data to eliminate distortions within uniform bottom areas.

The local polynomials method has been used for the smoothing and reconstruction of bedforms. This method is part of deterministic methods that assume the existence of analytical dependencies between values in space. The polynomials method of the deterministic group uses a polynomial defined at some point from its coordinates. For example, for a point i with coordinates (x, y) the function F (x, y) = P_n (x, y), where P_n is a polynomial of degree n can be applied. The first-order polynomials are used for the most common two-dimensional cases [34]. The local polynomial interpolation fits many polynomials, each within specified overlapping neighbourhoods, providing an accurate approximation for the points. This is a simple method devoid of bias that allows smoothing of local data microvariations and extreme values (usually noise) that are not common for the neighbourhood. Using this method allowed us to eliminate noise on the digital model surface with a 0.13 m root mean square error.

The System for Automated Geoscientific Analyses (SAGA) GIS was used to remove stripe artefacts by means of convolution filters [35,36], thus allowing preservation of the general angle exposition and reduction of error angles from the data array. Nevertheless, this approach did not provide for the creation of accurate bathymetric terrain models because the depth difference between the initial and resulting data was too large.

It is assumed that the "banding" was caused by incorrectly setting the tilt of the sonar head (HeadTilt) at 1 along with equipment error. There were no significant improvements or noticeable changes in data quality when processing the data using the PDS2000 software when values (e.g., roll 0

and −1) were changed. Temperature may have played a role in the failure as the recorded temperature in the echosounder menu (the temperature of the radiator is fixed at close to absolute zero) is a reliable error. A similar situation was not observed in the following surveys (September–October 2017).

Artefacts can limit the interpretation of morphometric properties when constructing DBMs. Band-shaped distortions form elongated shapes, which are more evident on flat surfaces of the sea bottom, resulting in erroneous characteristics of inclines and orientation of the seabed (Figure 3C). Elimination of such errors using the procedure of de-striping [35,36] allows the true slope to be kept (Figure 3D).

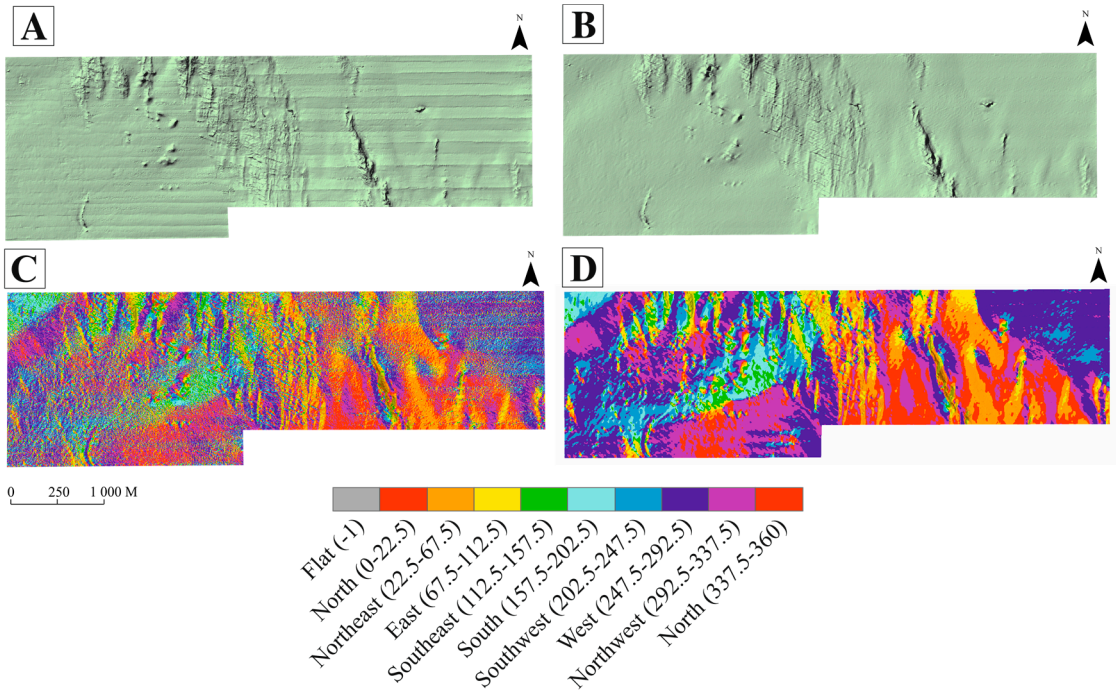

Figure 3. Orientation of the seabed calculated from the models (Moschny Island key area). (**A**) initial shaded relief prior to approximation; (**B**) shaded relied after approximating and de-striping; (**C**) initial seabed slope prior to approximation; (**D**) seabed representation after approximating and de-striping.

This process consisted of two main steps: (1) data cleaning with filters, and (2) post-processing and manual cleaning. Systematic depth distortions along with edge beam inaccuracies were removed by filtering the acquired bathymetric data. Non-systematic distortions were removed by manual processing.

2.5. GIS Analyses of Bottom Relief

GIS analyses of the seafloor bottom relief and the accompanying dataset of geophysical data were carried out using ArcGIS software. MBES data (at 3 m resolution) were used to calculate aspect, slope, and terrain ruggedness using ArcGIS Spatial Analyst and the Benthic Terrain Modeler toolbox (Figures 4–7). The software allowed the identification of specific geomorphological features, such as downslope direction, degrees of slope inclination, terrain ruggedness, and local relative relief of rises and depressions (Table 1) [37,38]. After processing and cleaning, digital terrain models (DTMs) were constructed in GIS, devoid of most artifacts. The regularity and coincidence of the artifacts with nadir made for easy identification of the artifacts. To calculate the Bathymetric Position Index (BPI), we used the Fine scale of the Bathymetric Position Index (BPI). To calculate the neighborhood, the inner radius used was 5 and the outer radius corresponded to 50. When calculating the aspect and slope, the default parameters were used.

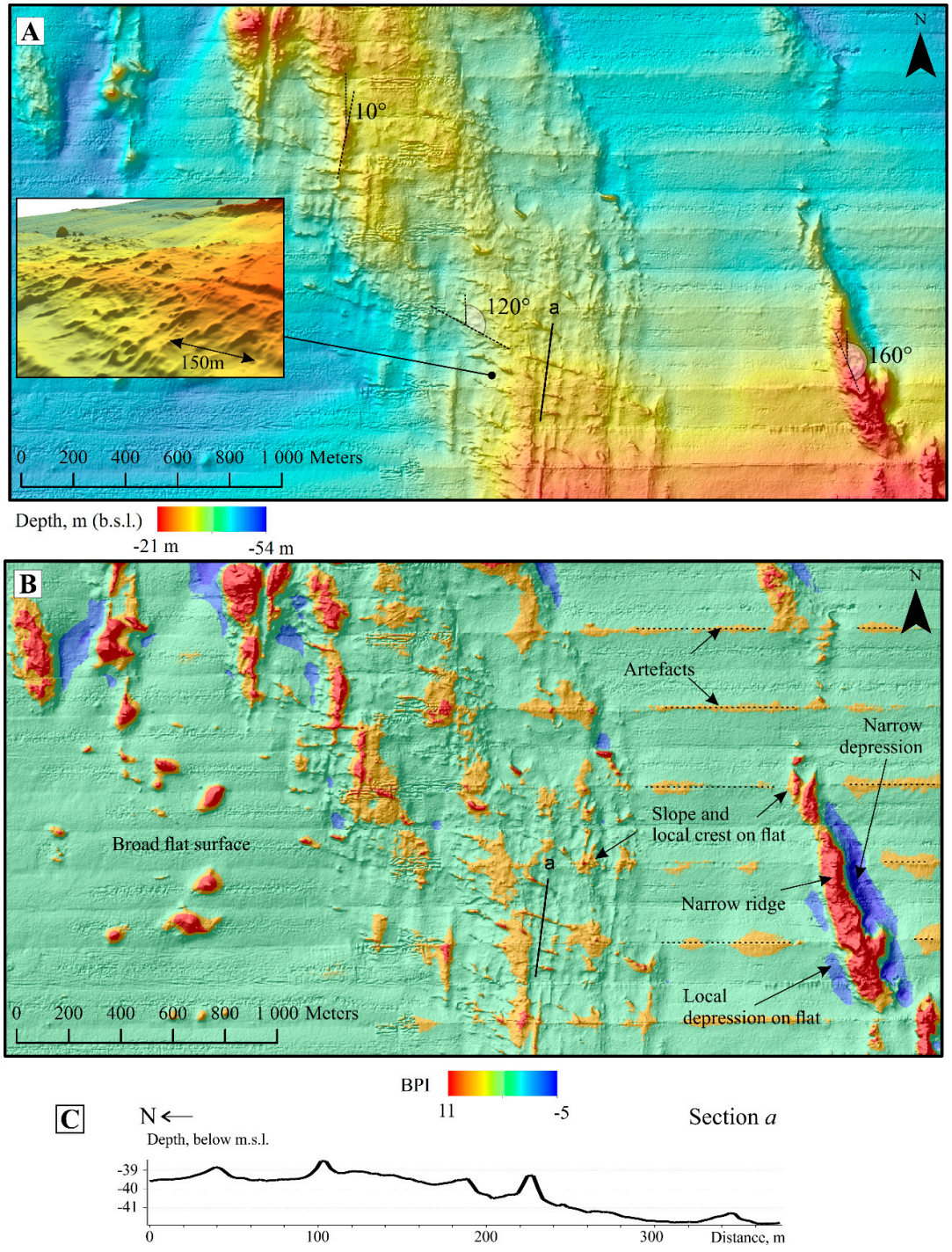

Figure 4. Digital bathymetric model (DBM) of the Moschny Island key area; (**A**) MBES image; (**B**) BPI map; (**C**) N–S oriented bathymetric profile constructed across small ridges.

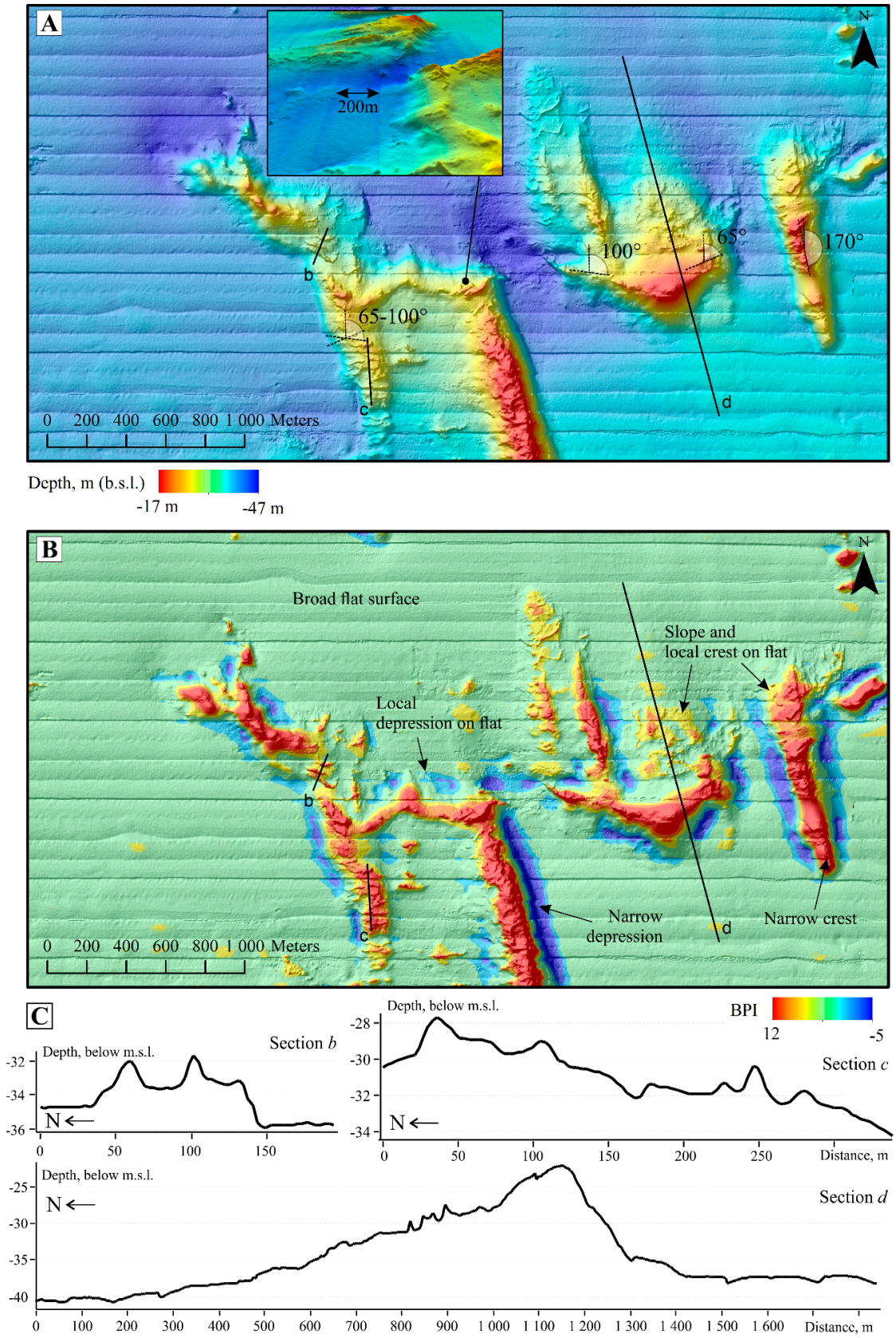

Figure 5. Digital bathymetric model (DBM) of the Vyborg Bay key area; (**A**) MBES image; (**B**) BPI; (**C**) bathymetric profiles across high relief forms.

Table 1. Results of morphometric analyses of MBES and SBP data.

Location	Shape	Direction (Azimuth)	Height Above Around Seafloor, m	Height of Ridge Above Its Base, m	Width of Ridge Base, m	Length of Ridge, m	Slope, Degrees	Crests Interval, m	Geological Interpretation
Isl. Moschny	Linear	NNE–SSW (10°)	0.5–1	-	20–60	1200	1–3°	-	Glacial erosion ridges
	Linear	SSE–NNW (160°)	5–8	15–20	100	1000	5–20°	-	Streamlined moraine ridges
	Linear	SE–NW (120°)	0.5–1.5	1–2	8–10	1300	5–15°	50–150 (av.85)	De Geer moraine
Vyborg Bay	Linear	SSE–NNW (170°)	10–15	15–20	130–170	1000	5–20°	-	Streamlined moraine ridges
	Crescent	NE–SW and SE–NW (65° and 100°)	10–20	10–25	from 70–200 to 300–1000	more than 4300	3–4° N slope 10° S slope	-	End-moraine ridges
	Crescent	NE–SW and SE–NW (65° and 100°)	0.5–1.5	1–2	8–10	300	5–20°	50	De Geer moraine

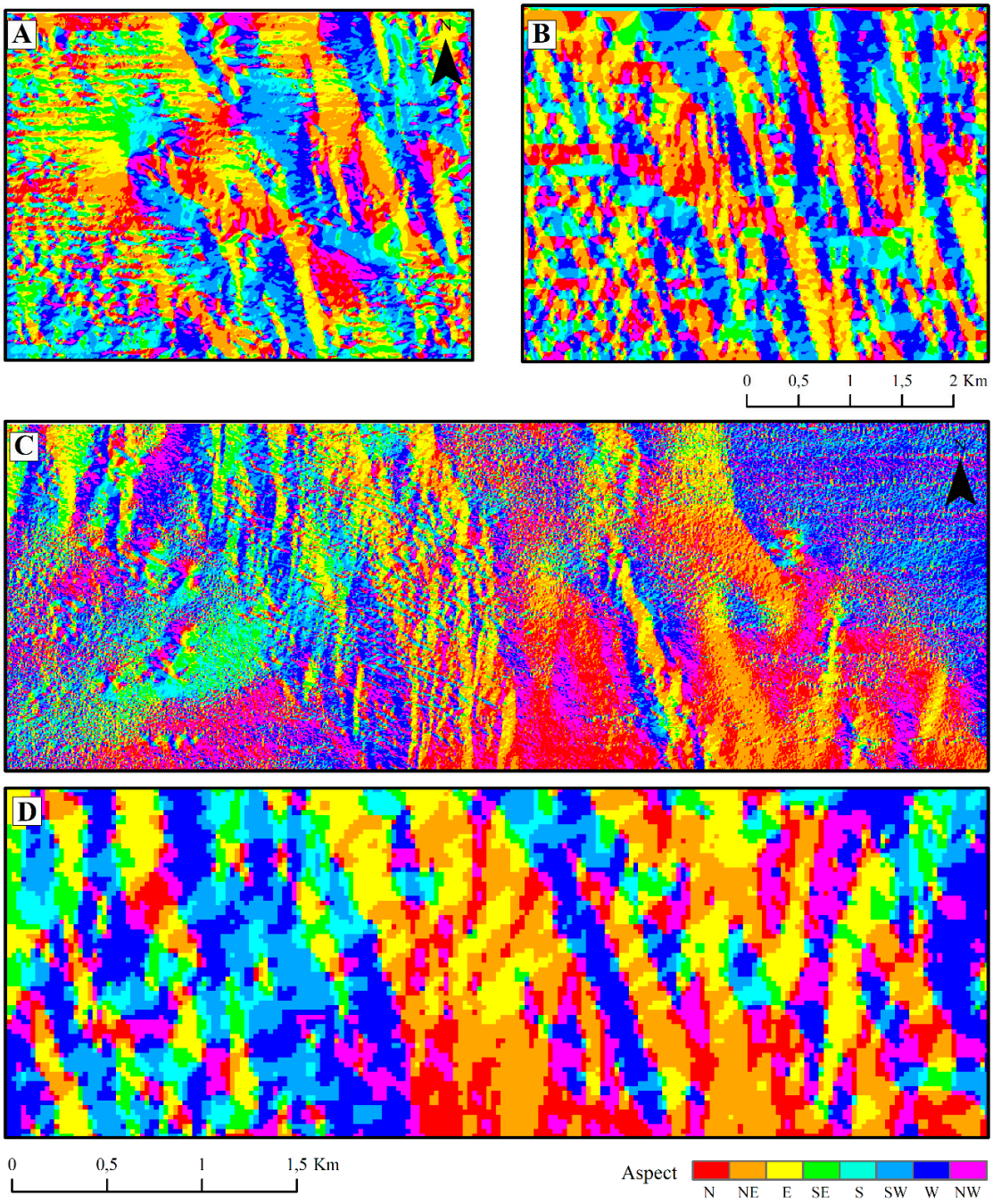

Figure 6. Aspect of slopes based on the MBES DBMs; (**A**) multibeam relief for the Vyborg key area, (**B**) glacial moraine surface of the Vyborg key area, (**C**) multibeam relief of the Moschny Island key area, (**D**) glacial moraine surface of the Moschny Island key area.

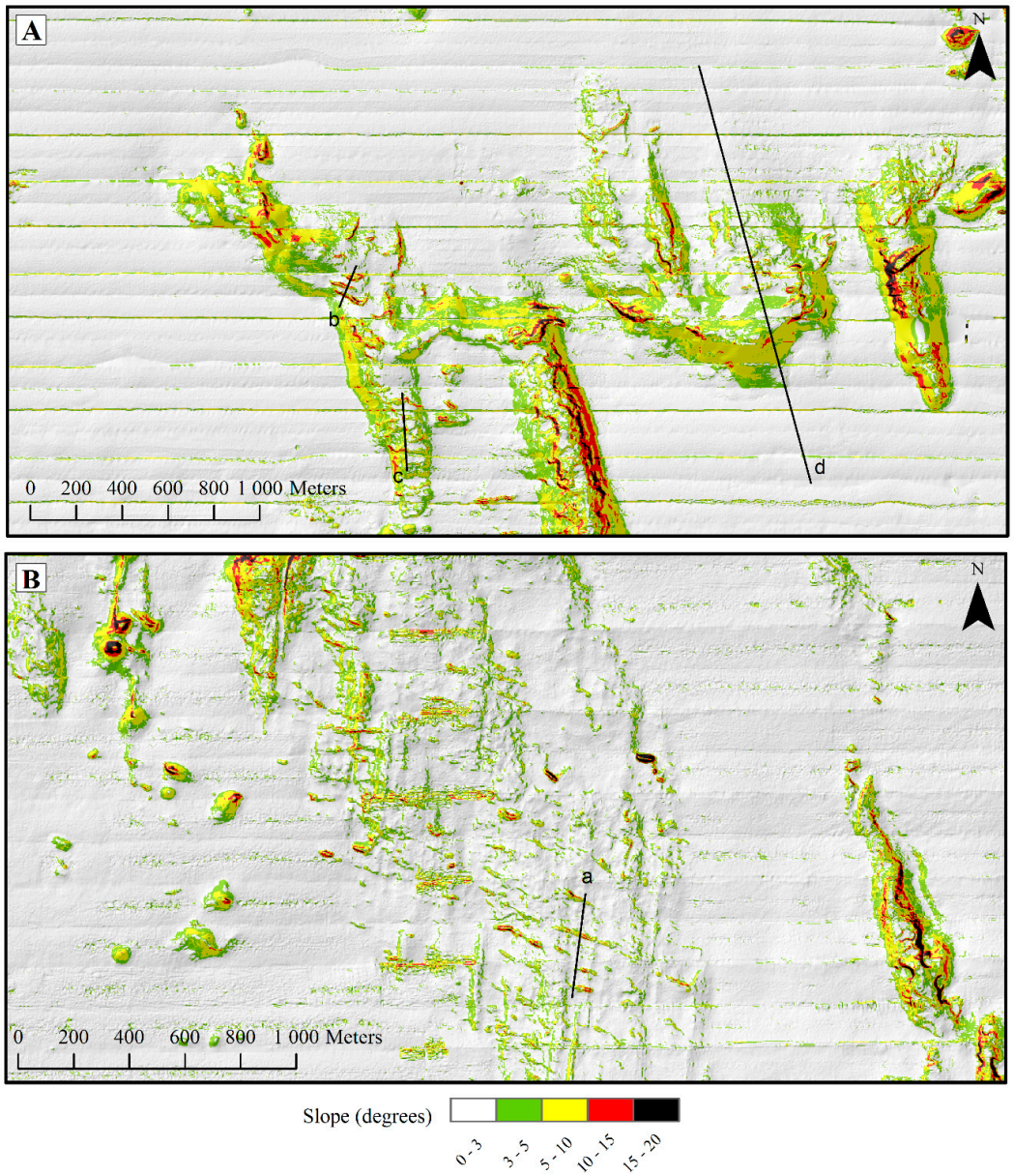

Figure 7. Slope in degrees (**A**) Moschny Island key area; (**B**) Vyborg key area. See Figures 5 and 6 for the locations of Profiles A–D. The colour ramp has been selected to highlight the main features of the terrain.

SBP Data Processing

The SBP data processing was carried out using RadExPro software. This software is commonly used for in-depth High/Ultra-high resolution (HR/UHR) marine seismic processing, real-time marine 2D/3D seismic quality control (QC), and complete processing of the shallow seismic-reflection data. Five distinct acoustic units were identified in the seismic-reflection SBP based on specific acoustic characteristics (Figure 8).

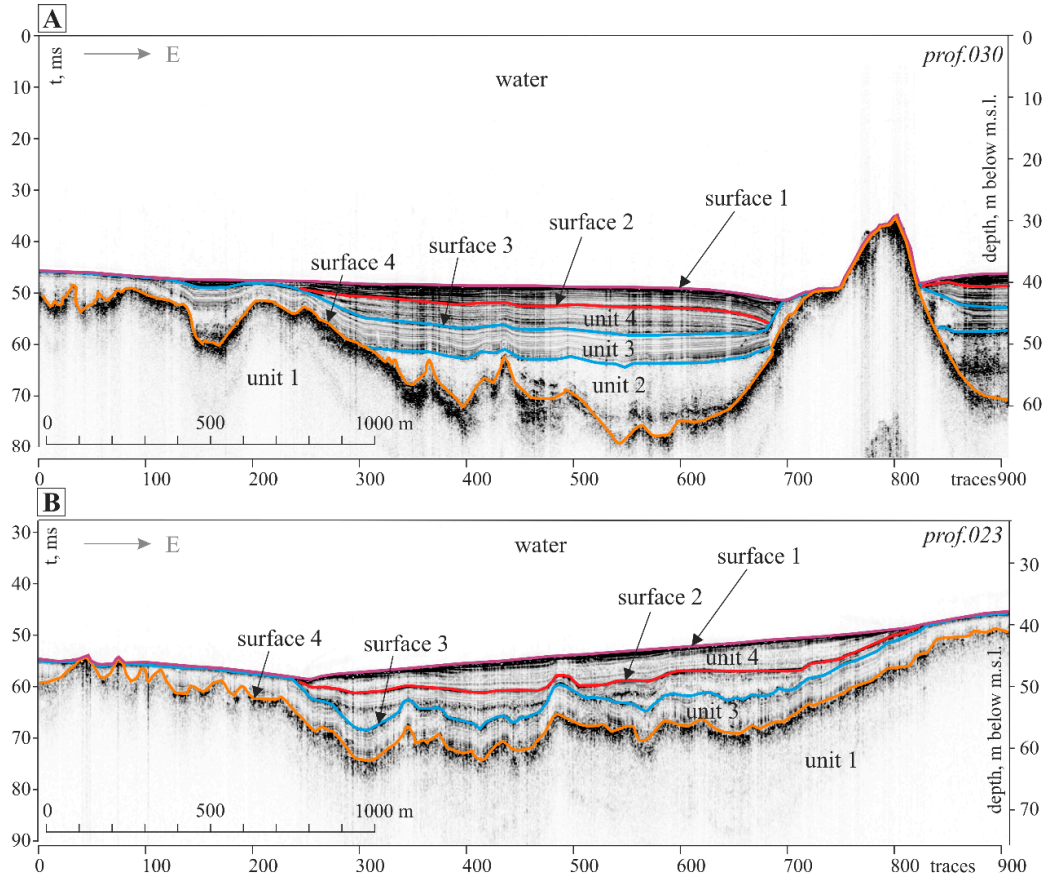

Figure 8. Seismic-reflection profiles: (**A**) Moschny Island key area (profile 023); (**B**) Vyborg Bay key area (profile 030). Interpreted acoustic units consist of Unit 1 = till (moraine); Unit 2 = questionably glaciofluvial sandy deposit; Unit 3 = Late Pleistocene glacio-lacustrine clays; Unit 4 = Holocene lacustrine and marine silty-clayey muds. Surface 1 = sea bottom surface; Surface 2 = inner erosion surface of Holocene mud; Surface 3 = top of Late Pleistocene clays; Surface 4 = top of till.

The upper limits of Unit 1 (Surface 4), Unit 3 (Surface 3), the seafloor (Surface 1), and the lower inner erosion boundary (Surface 2) were easily traced using the intensive axes of in-phase refractions of Unit 4. As a result, spread sheets that contain the geographic coordinates, and the absolute height of each point of the acoustic boundaries (surfaces) were constructed. These data were imported into ArcGIS 10.0 and interpolated with the Natural Neighbour method at 10-m cell size for the erosional boundary in Unit 4 and the top of Unit 3. All other surfaces were interpolated at a 25-m cell size. Border imaging was performed in ArcScene. The difference in window sizes is caused by array variety. Erosion surfaces have sub-horizontal relief, while the other surfaces have a rugged one. The density of the bottom relief data is high enough in all directions, and it allows interpolation, even with a smaller cell size, without any errors. Data about sub-bottom surfaces are redundant along the profile lines, but there is nothing between them to avoid the occurrence of error interpolation with a greater cell size. Using the tools "Aspect" and "Slope", transformations of the surfaces were accomplished to show the azimuth of sloping platforms and steepness of slopes (see Figure 6B,D).

The SBP data processing and interpolation was used to construct a 3D model of the distinct acoustic surfaces (see Figure 9). However, the resolution of this model is much lower than the bottom relief digital bathymetric model (DBM), but it provides some useful information that we feel is important for geological interpretation.

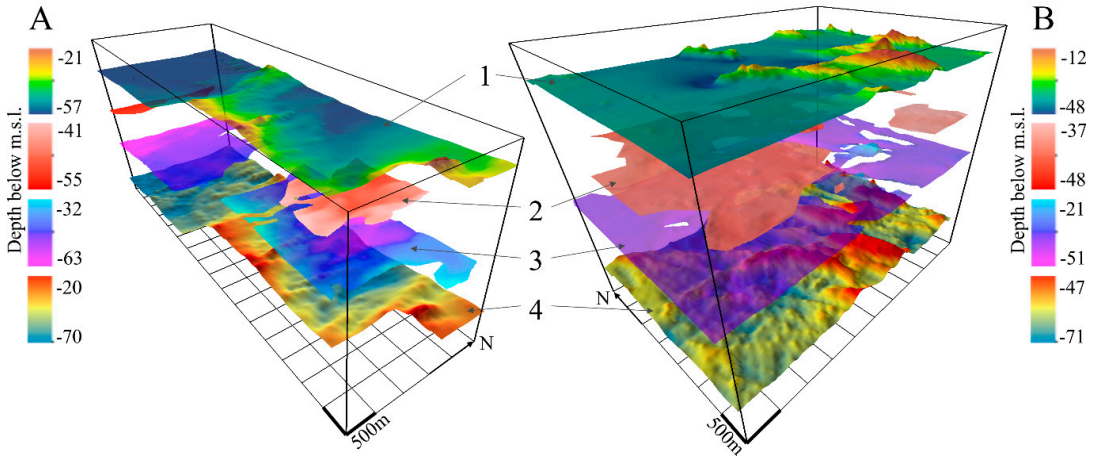

Figure 9. A 3D model of acoustic surfaces based on SBP processing; (**A**) Moschny Island key area, (**B**) Vyborg Bay key area. Geological interpretation of surfaces consists of: 1 = recent bottom surface, 2 = inner erosion surface of Holocene mud, 3 = surface of Late Pleistocene clays, 4 = till surface.

3. Results

The geological interpretation of the SBP and MBES data (see Figures 8 and 10) is based on the analyses of grab samples and gravity cores collected from Quaternary sediment from the geological surveys of the 1990s [13,14]. Although the cores' penetration depths were only 2 to 4 m, till, Late Pleistocene glacio-lacustrine clays, Holocene silty-clay, and mud were sampled from distinct seafloor exposures in the Eastern Gulf of Finland. All of these sedimentary units are characterized by a distinct lithologic composition and sedimentary structures that facilitates correlating them to our interpreted acoustic units with a high degree of confidence.

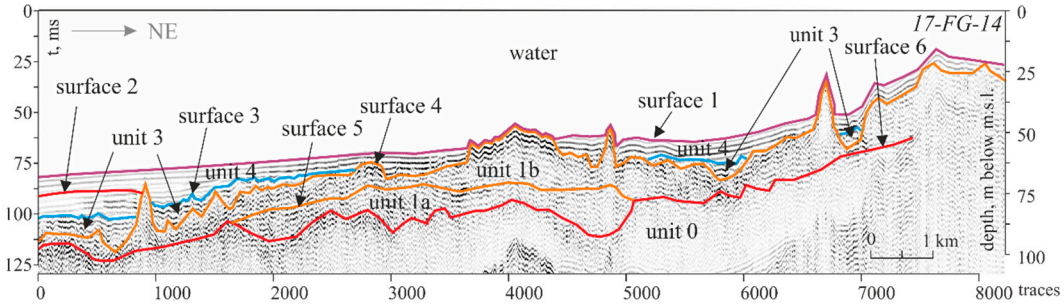

Figure 10. A seismic-reflection profile (17-FG-14) near the Moschny Island key area. Geological interpretation consists of Unit 0 = Vendian deposits, Unit 1a = lower till, Unit 1b = upper till, Unit 3 = Late Pleistocene glacio-lacustrine clays, and Unit 4 = Holocene lacustrine and marine silty-clayey muds. Surface 1 = sea bottom surface; Surface 2 = inner erosional horizon in Holocene mud, Surface 3 = top of Late Pleistocene clays, Surface 4 = top of till, Surface 5 = inner surface between two moraines. Surface 6 = top of Vendian deposits.

In the Vyborg Bay key area (see Figures 1A and 2A), the depth of the seafloor varies from 12 to 15 m along the crests of moraine ridges and between 35 to 40 m within the sedimentary basins. Figure 8B shows interpreted seismic-reflection profiles collected in the key area that exhibit separate and distinct acoustic characteristics. The top (Surface 4) of Unit 1 is characterized by discontinuous high-amplitude reflections lacking an explicit in-phase correlation. An acoustical transparent zone lacking reflections lies below Unit 1, which can be traced over the entire survey area. Unit 1 corresponds to the basal Quaternary sedimentary unit, which overlies the Vyborg complex of rapakivi granite–gabbroic anorthosites and is composed of 20 to 30 m thick tills deposited during

the last glaciation. Maximum thicknesses are found along moraine ridges. The results of our study present a much more complicated picture of moraine ridge distribution compared to that previously shown [17–19] (see Figures 2B and 11A).

Using the results from sediment sampling of exposed till (Unit 1) and the presence of numerous boulders on the seafloor, we were able to map the aerial extent of the till. In addition, we mapped specific seafloor depressions with depths <1 m associated with exposed moraine ridges whose encircling depressions result from contourite currents (Figure 11A).

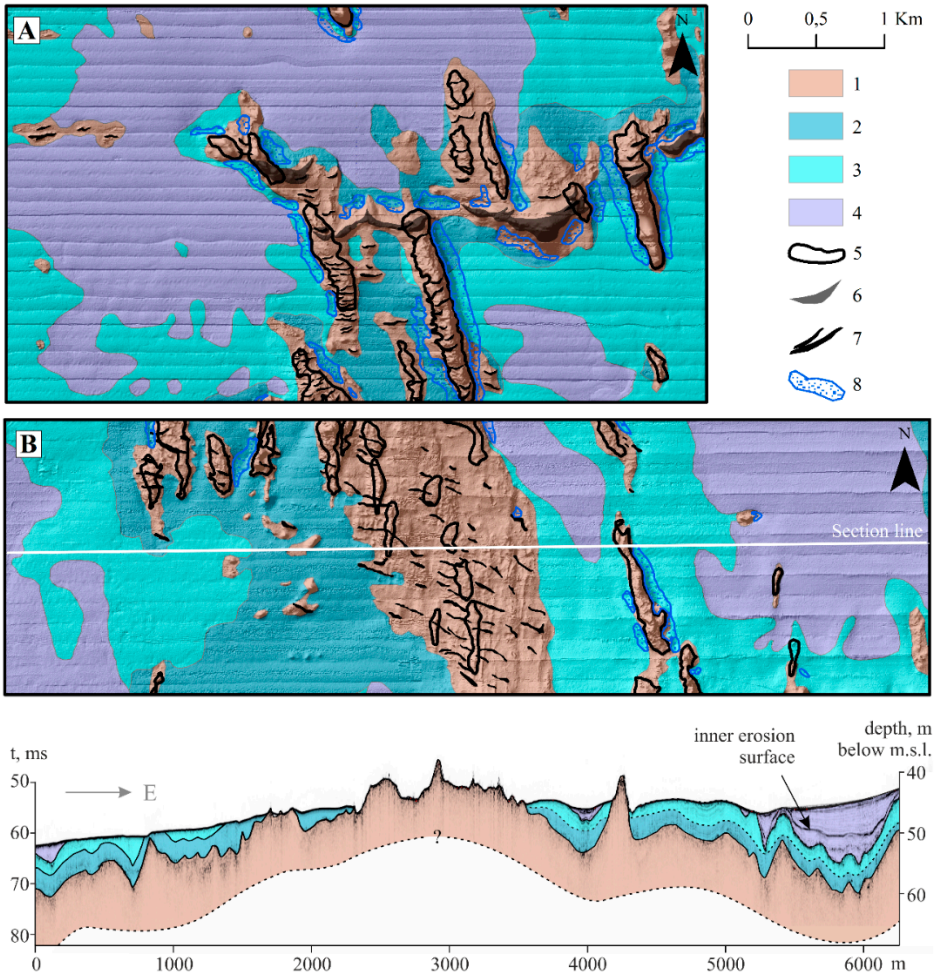

Figure 11. Distribution of Quaternary sedimentary units and seabed morphology based on geological interpretation of SBP and MBES data; (**A**) Vyborg Bay key area; (**B**) Moschny Island key area; (**C**) W–E cross-section. Sedimentary units (see explanation in panel A) consist of 1 = seafloor exposures of Late Pleistocene till with unconformable surface; 2 = seafloor exposures of Late Pleistocene varved glacio-lacustrine clays with unconformable surface; 3 = seafloor exposures of unconformable to disconformable Late Pleistocene homogenous (non-laminated) glacio-lacustrine clays, 4 = sediment basin filled with Holocene marine silty-clayey muds. Interpreted geomorphological features consist of 5 = streamlined moraine ridges; 6 = end-moraine ridges; 7 = De Geer moraine; 8 = depressions formed as a result of contourite current action around exposed moraine ridges.

Unit 3 exhibits parallel rhythmic reflections with in-phase axes of varying amplitudes in the seismic-reflection profiles that are conformable with the surface of the underlying acoustic unit (Figure 8B). Unit 3 is widely distributed in the key areas, and its upper-most reflection (Surface 3) is identified by a bright spot (high amplitude reflection), characteristic of the Late Pleistocene glacio-lacustrine varved and homogenous clays that accumulated in ice marginal lakes and the Baltic

Ice Lake. The exposed glacio-lacustrine clays are characterized in the MBES surface roughness images and can be divided into two types (Figure 11A): (1) a rough surface, interpreted as exposed varved clay (lower part of Unit 3) that formed due to selective removal of fine-grained material and enrichment of coarse-grained (gravel, pebbles) sediment, forming a surficial lag deposit; (2) the smoothed surface imaged from the MBES bathymetry is characteristic of homogeneous lacustrine-glacial outcrops. These outcrops are found in areas of little erosion or sediment starved areas. The thickness of the glacio-lacustrine clays ranges from 5 to 10 m.

Unit 4 represents Holocene Ancylus Lake and marine Littorina and Post-Littorina silty-clayey mud in the Vyborg Bay key area (Figure 8B). Here, sediment basins are filled with Holocene muds that dominate the seafloor in this key area (Figure 11A). Locally, mainly in the Northwestern part of the Vyborg Bay key area, acoustic Unit 4 is characterized by sub-horizontal, in-phase axes with variable amplitude reflections. Holocene marine muds >10 m fill local basins located in the Northwestern part of the key area (Figure 11A).

In the Moschny Island key area (Figures 1A, 2B and 11B) the seafloor is characterized by a relatively smooth surface that varies in depth from 54 m within the basins in the Western part, to 21 m on the crests of moraine ridges. In the south, near Moschny Island, depths are markedly shallower. Late Pleistocene varved and homogenous clays deposited in ice marginal lakes and the Baltic Ice Lake cover the seafloor in this key area, as reported from previous investigations [14]. Two local sedimentation basins filled by Holocene silty-clay mud are found in the Eastern and Western parts of the Moschny Island area (Figure 2B). The MBES survey data show a complicated distribution of Quaternary sediment and geomorphic features (Figure 11B).

Pre-Quaternary deposits in the Moschny Island key area are represented by Vendian sediment rocks [14]. The Quaternary basal unit (acoustic Unit 1) is represented by till (<25 m thick). Relative to the seafloor, depths of rare narrow depressions surrounding moraine ridges are up to 2 m deep. Locally above the tills, acoustically transparent zones occur within local depressions (Unit 2 in Figure 8A). The upper boundary of acoustic Unit 2 is sub-horizontal to the lower part of the overlying acoustic Unit 3. Unit 2 is up to 12 m thick. Unit 2 is not exposed in this key area and consequently was not sampled.

Acoustic Unit 3 is characterized by a series of parallel reflections of varying amplitudes, conformable with the reflections of the underlying unit (Figure 8A). This unit represents Late Pleistocene glacio-lacustrine clays that are widely distributed in the Moschny Island key area. As previously described for the Vyborg Bay key area, it is possible to divide outcrops of varved clays and homogenous clays using MBES (Figure 11B). The total thickness of the glacio-lacustrine deposits rarely exceed 6 to 8 m. Acoustic Unit 4 represents the Holocene lacustrine and marine silty-clay muds up to 10 m thick that have accumulated within local sediment basins.

Based on the MBES data, the DBMs of Moschny and Vyborg Bay areas were constructed to illustrate the results of our surveys (Figures 5 and 6). Aspect map analyses revealed several orientations of seafloor geomorphic features within both key areas. The primary orientation for well-defined, elongated, linear ridges up to 1000 m long, 100 to 170 m wide and 15–20 m high (Table 1, Figures 4 and 5) is SSE–NNW (160°–170°), observed on the till surface (Figure 7B,D). These ridges are characterized by the maximum degree of slope in the aspect map (Figure 7).

A secondary orientation is NNE–SSW (10°) for a less well-defined (than that observed for the primary orientation) bottom relief that represents linear elongations up to 1200 m long, 20 to 60 m wide and 0.5–1 m high (Table 1, Figure 4). These features are only observed within the Moschny Island key area (Figure 6C,D).

A tertiary orientation for bottom relief is SE–NW (120°), for small, 0.5 to 1.5 m (some up to 2 m) high, 8 to 10 m wide, and up to 1300 m long, rhythmic, parallel ridges, spaced from 50 to 150 m apart (Table 1, Figure 4). These features are prominent within relatively bathymetric high areas of the Moschny Island key area where they are characterized as interrupted linear features (Figure 6C). In the bathymetric low area, the ridges are subdued or absent. These features are not

exhibited in the till surface (Figures 6D and 9), most likely due to information being deleted during the processing of the DBM. This may be the result of interpolation caused by high data resolution along the seismic-reflection survey line and the absence of data between the survey lines [28]. However, very distinct individual ridge crests exhibited in the seismic-reflection profiles (Figure 8B) can be traced for quite a long distance (up to 1300 m) on the surface of a relatively flat bathymetric rise.

In the Vyborg Bay area, the >4300 m long curved bedforms, and those oriented roughly NE–SW to SE–NW (65° to 100°) can be traced on the till surface (Figure 7A,B). Morphologically, this orientation corresponds to relatively high (10–20 m) and wide (70–200 m to 300–1000 m) ridges (Table 1, Figure 5).

Small rhythmically-curved, lined bedforms of similar orientation are observed on the ridges' surfaces. These bedforms are 0.5 to 1.5 m (up to 2 m) high, 8 to 10 m wide and up to 300 m long (Table 1, Figure 5). In depressions, these ridges are not visible; thus they are not traced on the glacial moraine DBM (Figure 7A,B), but like in the Moschny key area, they can be identified on seismic-reflection profiles.

4. Discussion

Reconstruction of the Late Weichselian ice sheet retreat through the Eastern Gulf of Finland basin is still a problem. Morphological and chronological deglaciation markers are primarily located onshore [23,39–46]. A lack of data from the marine environment and existing contradictory hypotheses has led to large uncertainties in the reconstruction of the ice margin retreat within recently submerged areas [23], including the Eastern Gulf of Finland [16]. High resolution MBES and SBP data can provide important geomorphological indicators of the ice sheet retreat, which occurred between 13.8 and 13.3 ka BP (Pandivere–Neva stage in the Southern coast of the gulf) [36,38] and 12.25 ka BP (Salpausselkä I stage, Southeastern Finland) [40,41].

The MBES and SBP data collected in 2017 and reported herein represent the first set of high resolution bathymetric data for the Eastern Gulf of Finland obtained for scientific study. These data provide a unique opportunity to describe and map significant small relief bedforms. The geological interpretations we present here are sound, even though not all artifacts in the MBES data could be removed. Since the seismic-reflection profiles were collected along the nadir of the MBES lines, morphometric analyses were validated with a high degree of confidence.

The dominant seafloor geomorphology in the Eastern Gulf of Finland are the 1000 m long, 100 to 170 m wide and 15 to 20 m high SSE–NNW (160°–170°) oriented elongated linear oval-shaped ridges, interpreted as streamlined moraine ridges and classified as drumlins. These features formed beneath an ice sheet as it moved over the land, parallel to the ice direction and are composed of basal till or lodgement till [45–47].

The 10 to 20 m high, 70 to 1000 m wide, approximately 4300 m long crescent ridge, oriented NE–SW to SE–NW (65°–100°), mapped in Vyborg Bay, is interpreted as an end-moraine, parallel to the terminal ice margin. Its asymmetrical shape (Figure 5C, section d) with the steeper (10° dipping) Southern (lee-side) and gentler (3–4°) Northern (stoss-side) slopes is characteristic of typical end-moraine morphology [45–47]. Although the general location of the end-moraine was predicted based on broad-scale bottom relief in previous GIS analyses [16], the precise location and morphological evidence was not known until our study. The end-moraine ridges that we have mapped are smaller in comparison to the Pandivere–Neva and Salpausselkä I glacial forms. The Pandivere–Neva terminal moraine zone consists of a curved and interrupted belt of push end-moraines, glaciofluvial deltas and eskers [48]. The heights of these features range from only a few metres up to 20 m [49], because Holocene wave erosion has substantially levelled them. In contrast, the Salpausselkä I moraine is 0.5 to 4 km wide and is approximately 20 to 80 m high [50,51].

Among the most interesting submerged glacial relief features found in our study are series of rhythmic parallel ridges, 1 to 1.5 m high, elongated at a slightly different direction within our two study areas. These ridges are overlaid with both drumlin and end-moraines. The small parallel ridges can be identified as De Geer moraines, which are typically described as relatively low till ridges,

with rhythmic parallel linear to curved positive relief features in plain view. Such clusters of de Geer moraines, with dimensions of <5 m high, 10 to 50 m wide, and >100 m long, are exemplified in the Replot and Björkö areas of the Kvarken Archipelago in Finland [45–47]. On the Northern slope of Slupsk Bank in the Southwestern Baltic, De Geer moraines exhibit ridges from 2 to 8 m high with a distance of 200 to 500 m between crests [52]. On the German Bank of the Southern Scotian Shelf of Atlantic Canada [53], the De Geer moraine is represented by sub-parallel ridges, varying from 1.5 m high and 40 m wide to 5 to 8 m high and 100 to 130 m wide. Individual ridges can be traced horizontally for a few hundred metres up to almost 10 km [53]. Numerous closely spaced linear and curvilinear ridges occur east of Shetland. The range of the ridges varies from 1 to 20 km in length, with distances from 700 to 2000 m. Most ridges have a vertical seafloor expression of between 10 and 20 m. These straight, sub-parallel, sharp-crested glacial features are interpreted as De Geer-type moraines [54]. Recent hypotheses on the origin of De Geer moraines are presented here. A study on the Kvarken Archipelago [45,47] proposed that the moraine there was formed in crevasses running parallel to the ice margin and deposited under sub-aquatic conditions. A study of the De Geer moraine on the German Bank indicated that its formation was at the grounding line of a tidewater glacier, the result of deposition and/or pushing action during minor re-advances, and and stillstands [53]. Therefore, a De Geer moraine reflects the probable position of a retreating ice margin. The MBES data collected in Vyborg Bay support this hypothesis as the direction of De Geer moraine coincides with elongation of the end-moraine ridge crest in Vyborg Bay.

A slight difference in orientations of the De Geer moraines mapped near Moschny Island and in Vyborg Bay indicates a rotation of the ice margin front during deglaciation, validating an earlier hypothesis [16,55]. However, this MBES study identified and comprehensively mapped De Geer moraines in the Eastern Gulf of Finland for the first time, even though an extensive SBP coverage had previously been done.

The low linear ridges located north of Moschny Island and oriented NNE–SSW (10°) were difficult to interpret. Acoustic units, interpreted as glacial moraine in seismic-reflection profiles (see profile 17-FG-14, Figure 10 for example), are different from the acoustically chaotic reflections absent of continuous reflections that generally characterize moraines. In profile 17-FG-14, well-defined, but irregular, reflections (e.g., Surface 5 of Figure 10) are interpreted to represent a reflection within the moraine units. The lower section (Unit 1a) of the moraine deposits appears to have been eroded by an overlying advancing glacier, followed by the deposition of another (upper) moraine deposit (Unit 1b).

Acoustic Surface 4 (Figure 8) is interpreted as the upper surface of till. Till, identified within both key areas, is mostly overlaid by a 5 to 7 m thick layer of varved clays, a rhythmic pair of brown clay layers and grey silty-microlayers [56]. The varved clays are very well identified in the seismic-reflection profiles (lower part of Unit 3, Figures 8 and 10) due to their laminated stratigraphy and "clothing" bedding. Homogeneous glacio-lacustrine clays, as determined from sediment core analyses [14,56], form the upper part of acoustic Unit 3 (Figures 8 and 10). Generally, in the Eastern Gulf of Finland, the boundary between typical varved clays and homogeneous clay is a facies transition. Locally, in the troughs of the moraine surface, between the till and the glacio-lacustrine deposits, there is a layer of sediment that appears to be glacio-fluvial sand (unit 2, Figure 8).

Another sharp erosive contact is exhibited as Surface 3 (Figure 8), which is proposed to lie between Late Pleistocene and Holocene sediments. Locally, erosion was so intense that up to 10 m of the Late Pleistocene glacio-lacustrine clays were eroded. This interpretation supports the interpretations made from other acoustic-seismic profiles [13,56], which support the hypothesis of a deep and relatively long period of low water level in the Eastern Gulf of Finland during the Early Holocene [57,58]. The general trend of relief transformation between the final stage of the ice sheet retreat and the beginning of the Holocene is relief smoothing as a result of glacio-fluvial and glacio-lacustrine sedimentation in the Late Pleistocene and intense submarine erosion after the final draining of the Baltic Ice Lake (Figures 8 and 9).

The distribution and thickness of Holocene silty-clay mud within the study area indicates a drastic change in the sedimentation processes since the beginning of the Ancylus Lake stage. Since that time,

accumulation has occurred within local sedimentary basins, while large areas in the Gulf of Finland were sediment-starved or experiencing erosion. Recent silty-clayey mud accumulation in the Eastern Gulf of Finland occurs in local sedimentary basins staggered along a ladder-shape bottom profile that steps down from a depth of 5 to 6 m in Neva Bay, to 80 m south of Gogland Island and is separated by vast sediment-starved or eroding areas (Figure 12). Three-dimensional geological models of our key areas and SBP data demonstrate that Holocene marine mud sedimentation occurred within local depressions at depths from 40 to 45 m in the Eastern part of the Moschny Island key area, and from 55 to 60 m in Vyborg Bay and the Western Moschny Island area. The thickness of the Holocene clayey mud varies from tens of cm on the slopes of ridges to 8 to 10 m in the deepest part of the sedimentary basins.

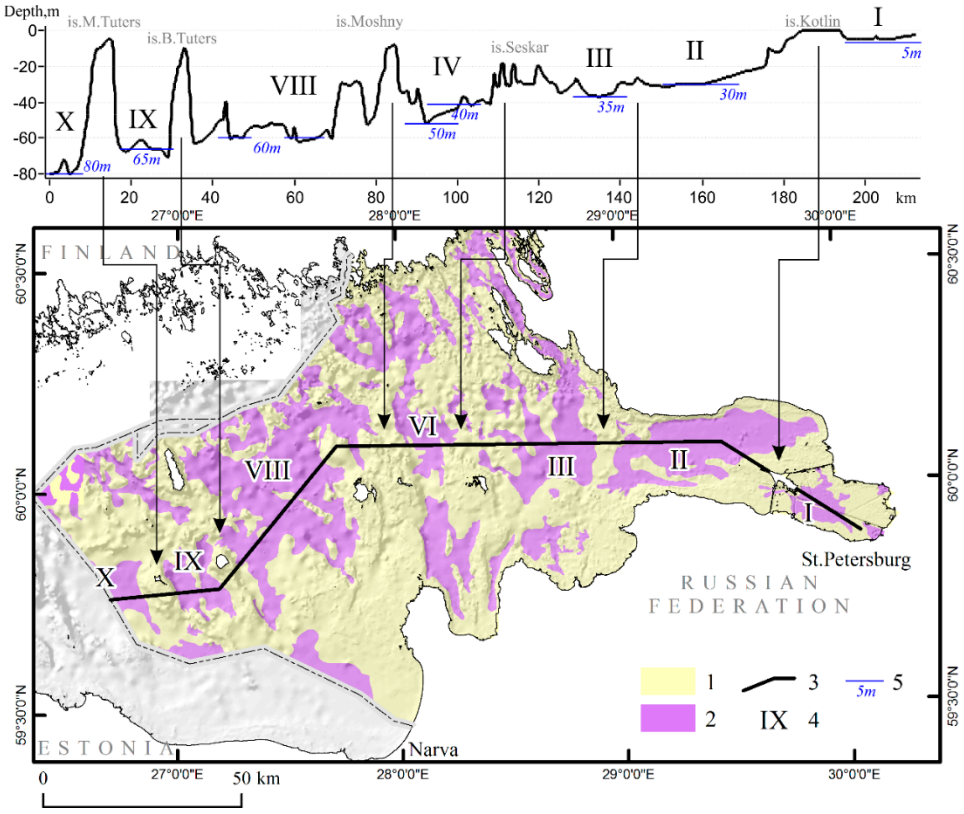

Figure 12. Schematic representation of the sedimentary basins in the Eastern Gulf of Finland: 1 = areas of submarine erosion and non-sedimentation, 2 = sediment basins with silty-clayey mud accumulation, 3 = cross-section profile line, 4 = sedimentary basin number, 5 = mean level of the modern clayey mud surface. Sediment basins are located along a ladder-shape profile, which steps down from depths of 5 to 6 m in the Neva Bay to 80 m south of Gogland Island and is separated by vast areas of non-sedimentation and erosion.

Our interpretation of the seismic-reflection profiles fixes one to two erosional surfaces within the Holocene mud. Construction of a 3D geological model allowed us to identify an erosional horizon within the muds that could be traced through all sedimentary basins within our study area at a depth of 45 to 60 m (Figure 9). We interpret the erosion to have taken place during a time of decreased water level. A lower water level in pre-Littorina time is supported by high-resolution sediment core investigations [15], modelling of submarine terrace formation [57], and onshore geoarcheological research [59]. More detailed study of Littorina sea-level fluctuations requires the continuation of high-resolution sediment coring.

5. Conclusions

1. Geophysical research in key areas of Vyborg Bay and north of Moschny Island using high-resolution MBES and SBP data revealed, for the first time, well-defined streamlined moraine ridges, De Geer moraines, and end-moraine ridges. Mapping of these glacial features established the location and orientation of the ice sheet margins during different stages of deglaciation in the Eastern (Russian) Gulf of Finland.
2. Our interpretations of high-resolution seismic-reflection profiles and 3D models of the till surfaces, Late Pleistocene sediments, and the mapping of the modern seafloor relief indicate that a significant fall in the water level in the Early Holocene and that, most likely, several water-level fluctuations occurred, documented by erosion surfaces (acoustic unconformable horizons) in silty-clay mud.
3. We conclude that the distribution and thickness of Holocene silty-clay mud mapped within our study areas indicates a drastic change in sedimentation since the beginning of the Ancylus Lake stage. Since the Ancylus, accumulation occurred within local sedimentary basins, while conditions of large bottom areas of the Gulf of Finland remained starved of sediment or suffered from erosion. Modern silty-clay accumulation in the Eastern Gulf of Finland occurs in local sedimentary basins, located at depths from 5 to 6 m in Neva Bay, to 80 m south of Gogland Island, which are separated by vast sediment starved and/or erosional areas.

Acknowledgments: Multibeam data processing was supported by the state assignment No. 0149-2018-0012. Data analyses and interpretation was carried out under project No. 17-77-20041 of Russian Science Foundation. The authors thank H. Gary Greene for helpful and important comments and language revision.

Author Contributions: The drafting of the research program, the primary processing of multibeam echosounder data in the software package PDS2000 and a description of the methods for obtaining and processing primary data was undertaken by Krek Alexander. The registration of primary MBES data and primary processing of the data array in the software package PDS2000 was accomplished by Kapustina Maria. The registration of the primary data for the upper sediment layer characterized in the SBP and the primary processing of the bathymetric data array in the PDS2000 software package was done by Tkacheva Elena. Danchenkov Aleksandr completed the final processing of bathymetric survey data in ArcGIS and SAGAGIS, including the elimination of artifacts in the digital models. He also contributed text for the section on research methods. Processing of seismic-reflection profiles was carried out by Budanov Leonid and Moskovtsev Alexandr. Geological interpretation was undertaken by Ryabchuk Daria, Sergeev Alexander and Zhamoida Vladimir.

Conflicts of Interest: The authors declare no conflict of interest.

References

1. Harff, J.; Björck, S.; Hoth, P. *The Baltic Sea Basin: Introduction. The Baltic Sea Basin Central and Eastern European Development Studies (CEEDES)*; Springer: Berlin/Heidelberg, Germany, 2011; pp. 3–9.
2. Uścinowicz, S. *Geochemistry of the Baltic Sea Surface Sediments*; Polish Geological Institute—National Research Institute: Warsaw, Poland, 2011; p. 356. ISBN 978-83-7538-814-5.
3. Kaskela, A.; Rousi, H.; Ronkainen, M.; Orlova, M.; Babin, A.; Gogoberidze, G.; Kostamo, K.; Kotilainen, A.; Neevin, I.; Ryabchuk, D.; et al. Linkages between benthic assemblages and physical environmental factors: The role of geodiversity in Eastern Gulf of Finland ecosystems. *Cont. Shelf Res.* **2017**, *142*, 1–13. [CrossRef]
4. Uścinowicz, S. *Relative Sea Level Changes, Glacio-Isostatic Rebound and Shoreline Displacement in the Southern Baltic*; Polish Geological Institute: Warsaw, Poland, 2003; Volume 10, p. 79.
5. Lampe, R.; Meter, H.; Ziekur, R.; Janke, W.; Endtmann, E. Holocene Evolution of the Irregularly Sinking Baltic Sea Coast and the Interactions of the Sea-Level Rise, Accumulation Space and Sediment Supply. In *SINCOS–Sinking Coasts. Geosphere, Ecosphere and Anthroposhere of the Holocene Southern Baltic Sea*; Harff, J., Luth, F., Eds.; Bericht der Romisch-Germanischen Kommission; Philipp von Zabern: Darmstadt, Germany, 2007; pp. 15–46.
6. Harff, J.; Meyer, M. *Coastlines of the Baltic Sea–Zones of Competition Between Geological Processes and a Changing Climate: Examples from the Southern Baltic*; The Baltic Sea Basin Central and Eastern European Development Studies (CEEDES) Book Series; Springer: Berlin/Heidelberg, Germany, 2011; pp. 149–164.

7. Hyttinen, O.; Kotilainen, A.T.; Virtasalo, J.J.; Kekäläinen, P.; Snowball, I.; Obrochta, S.; Andrén, T. Holocene stratigraphy of the Ångermanälven River estuary, Bothnian Sea. *Geo-Mar. Lett.* **2016**, *37*, 273–288. [CrossRef]
8. Gordeeva, S.; Malinin, V. *Gulf of Finland Sea Level Variability*; RSHU Publishers: St. Petersburg, Russia, 2014; p. 179. ISBN 978-5-86813-403-6. (In Russian)
9. Rosentau, A.; Veski, S.; Kriiska, A.; Aunap, R.; Vassiljev, J.; Saarse, L.; Hang, T.; Heinsalu, A.; Oja, T. *Palaeogeographic Model for the SW Estonian Coastal Zone of the Baltic Sea*; The Baltic Sea Basin Central and Eastern European Development Studies (CEEDES) book series; Springer: Berlin/Heidelberg, Germany, 2011; pp. 165–188.
10. Rosentau, A.; Muru, M.; Kriiska, A.; Subetto, D.A.; Vassiljev, J.; Hang, T.; Gerasimov, D.; Nordqvist, K.; Ludikova, A.; Lõugas, L.; et al. Stone Age settlement and Holocene shore displacement in the Narva-Luga Klint Bay area, eastern Gulf of Finland. *Boreas* **2013**, *42*, 912–931. [CrossRef]
11. Sandgren, P.; Subetto, D.A.; Berglund, B.E.; Davydova, N.N.; Savelieva, L.A. Mid-Holocene Littorina Sea transgressions based on stratígraphíc studies in coastal lakes of NW Russia. *GFF* **2004**, *126*, 363–380. [CrossRef]
12. Miettinen, A.; Savelieva, L.; Subetto, D.; Dzhinoridze, R.; Arslanov, K.; Hyvärinen, H. Palaeoenvironment of the Karelian Isthmus, the easternmost part of the Gulf of Finland, during the Litorina Sea stage of the Baltic Sea history. *Boreas* **2007**, *36*, 441–458. [CrossRef]
13. Ryabchuk, D.; Zhamoida, V.; Amantov, A.; Sergeev, A.; Gusentsova, T.; Sorokin, P.; Kulkova, M.; Gerasimov, D. Development of the coastal systems of the easternmost Gulf of Finland, and their links with Neolithic–Bronze and Iron Age settlements. *Geol. Soc. Lond. Spec. Publ.* **2016**, *411*, 51–76. [CrossRef]
14. Petrov, O.V. *Atlas of Geological and Geoecological Maps of the Russian Part of the Baltic Sea*; VSEGEI: St. Petersburg, Russia, 2010; 78p.
15. Virtasalo, J.J.; Ryabchuk, D.; Kotilainen, A.T.; Zhamoida, V.; Grigoriev, A.; Sivkov, V.; Dorokhova, E. Middle Holocene to present sedimentary environment in the easternmost Gulf of Finland (Baltic Sea) and the birth of the Neva River. *Mar. Geol.* **2014**, *350*, 84–96. [CrossRef]
16. Ryabchuk, D.; Hyttinen, O.; Zhamoida, V.; Kotilainen, A.; Sergeev, A.; Amantov, A.; Budanov, L.; Moskovtsev, A. Deglaciation of the Eastern Gulf of Finland basin. Unpublished manuscript. 2017.
17. Krasnov, I.I.; Duphorn, K.; Voges, A. (Eds.) *International Quaternary Map of Europe 1:2,500,000*; Sheet 3, Nordkapp; UNESCO: Hanover, Germany, 1971.
18. Zarina, E.P. Geochronology and Paleogeography of Late Pleistocene of the North-West of Russia. In *Periodization and Paleogeography of Late Pleistocene*; VSEGEI: Leningrad, Soviet Union, 1970; pp. 27–33. (In Russian)
19. Kvasov, D.D. *Late Quaternary History of the Large Lakes and Inner Seas of the Eastern Europe*; Nauka: Leningrad, Russia, 1975; p. 278. (In Russian)
20. Raukas, A.; Hyvärinen, H. (Eds.) *Geology of the Gulf of Finland*; Valgus: Tallinn, Estonia, 1991; p. 422.
21. Subetto, D.A. *Lake Sediments: Paleolimnological Reconstructions*; Herzen Russian State Pedagogical University: St. Petersburg, Russia, 2009; p. 339. ISBN 978-5-8064-1444-2. (In Russian, resume in English).
22. Vassiljev, J.C.B.C.; Saarse, L.; Rosentau, A. *Palaeoreconstruction of the Baltic Ice Lake in the Eastern Baltic*; The Baltic Sea Basin Central and Eastern European Development Studies (CEEDES) Book Series; Springer: Berlin/Heidelberg, Germany, 2011; pp. 189–202.
23. Hughes, A.L.C.; Gyllencreutz, R.; Lohne, Ø.S.; Mangerud, J.; Svendsen, J.I. The last Eurasian ice sheets—A chronological database and time-Slice reconstruction, DATED-1. *Boreas* **2016**, *45*, 1–45. [CrossRef]
24. Dorschel, B.; Wheeler, A.J.; Monteys, X.; Verbruggen, K. *On the Irish Seabed. Atlas of the Deep-Water Seabed*; Springer: New York, NY, USA, 2010; p. 164.
25. Harris, P.T.; Baker, E.K. *GeoHab Atlas of Seafloor Geomorphic Features and Benthic Habitats. Seafloor Geomorphology as Benthic Habitat*; Elsevier: Amsterdam, Netherlands, 2012; pp. 871–890.
26. Diesing, M.; Green, S.L.; Stephens, D.; Lark, R.M.; Stewart, H.A.; Dove, D. Mapping seabed sediments: Comparison of manual, geostatistical, object-based image analysis and machine learning approaches. *Cont. Shelf Res.* **2014**, *84*, 107–119. [CrossRef]
27. Dove, D.; Arosio, R.; Finlayson, A.; Bradwell, T.; Howe, J.A. Submarine glacial landforms record Late Pleistocene ice-Sheet dynamics, Inner Hebrides, Scotland. *Quat. Sci. Rev.* **2015**, *123*, 76–90. [CrossRef]

28. Lecours, V.; Dolan, M.F.J.; Micallef, A.; Lucieer, V.L. A review of marine geomorphometry, the quantitative study of the seafloor. *Hydrol. Earth Syst. Sci.* **2016**, *20*, 3207–3244. [CrossRef]
29. Flemming, N.C.; Harff, J.; Moura, D.; Burgess, A.; Bailey, G.N. (Eds.) *Submerged Landscapes of the European Continental Shelf*; John Wiley & Sons, Inc.: Hoboken, NJ, USA, 2017; p. 533. ISBN 9781118922132.
30. Petrov, O.V.; Lygin, A.M. (Eds.) *Information Bulletin on Geological Environment Assessment of the Near-Shore Areas of the Barents, White and Baltic Seas*; VSEGEI: St. Petersburg, Russia, 2014; p. 136. (In Russian)
31. Raateoja, M.; Setälä, O. *The Gulf of Finland Assessment*; Reports of the Finnish Institute Series; Finnish Environment Institute: Helsinki, Finland, 2016; Volume 27, p. 363.
32. Zhamoida, V.; Grigoriev, A.; Ryabchuk, D.; Evdokimenko, A.; Kotilainen, A.T.; Vallius, H.; Kaskela, A.M. Ferromanganese concretions of the eastern Gulf of Finland–Environmental role and effects of submarine mining. *J. Mar. Syst.* **2017**, *172*, 178–187. [CrossRef]
33. Sibson, R. Chapter 2: A Brief Description of Natural Neighbor Interpolation. In *Interpolating Multivariate Data*; John Wiley & Sons: New York, NY, USA, 1981; pp. 21–36.
34. Demyanov, V.; Savelyeva, E. *Geostatistics: Theory and Practice*; Nauka: Moscow, Russia, 2010; p. 327. ISBN 978-5-02-037478-2.
35. Oimoen, M.J. An Effective Filter for Removal of Production Artifacts in U.S. Geological Survey 7.5-Minute Digital Elevation Models. In Proceedings of the Fourteenth International Conference on Applied Geologic Remote Sensing, Las Vegas, NV, USA, 6–8 November 2000; pp. 311–319.
36. Peregro, A. SRTM DEM Destriping with SAGA GIS: Consequences on Drainage Network Extraction. Available online: http://www.webalice.it/alper78/saga_mod/destriping/destriping.html (accessed on 7 December 2017).
37. Wright, D.J.; Lundblad, E.R.; Larkin, E.M.; Rinehart, R.W.; Murphy, J.; Cary-Kothera, L.; Draganov, K. ArcGIS Benthic Terrain Modeler. Available online: http://www.csc.noaa.gov/products/btm/ (accessed on 20 January 2017).
38. Lundblad, E.; Wright, D.J.; Miller, J.; Larkin, E.M.; Rinehart, R.; Battista, T.; Anderson, S.M.; Naar, D.F.; Donahue, B.T. A benthic terrain classification scheme for American Samoa. *Mar. Geod.* **2006**, *29*, 89–111. [CrossRef]
39. Bulletin de la Commission Pour L'etude du Quaternaire. Available online: http://ginras.ru/library/pdf/2_1930_bull_quatern_comission.pdf (accessed on 10 November 2017).
40. Donner, J. *The Quaternary History of Scandinavia*; Cambridge University Press: London, UK, 1995; p. 200. ISBN 978-0-521-01831-9.
41. Saarnisto, M.; Saarinen, T. Deglaciation chronology of the Scandinavian Ice Sheet from the Lake Onega Basin to the Salpausselkä End Moraines. *Glob. Planet. Chang.* **2001**, *31*, 387–405. [CrossRef]
42. Hang, T. A local clay-Varve chronology and proglacial sedimentary environment in glacial Lake Peipsi, eastern Estonia. *Boreas* **2003**, *32*, 416–426. [CrossRef]
43. Kalm, V. Pleistocene chronostratigraphy in Estonia, southeastern sector of the Scandinavian glaciation. *Quat. Sci. Rev.* **2006**, *25*, 960–975. [CrossRef]
44. Vassiljev, J.; Saarse, L. Timing of the Baltic Ice Lake in the eastern Baltic. *Bull. Geol. Soc. Finl.* **2013**, *85*, 9–18. [CrossRef]
45. Breilin, O.; Kotilainen, A.; Nenonen, K.; Virransalo, P.; Ojalainen, J.; Stén, C.-G. Geology of the Kvarken Archipelago. Appendix 1 to the application for nomination of the Kvarken Archipelago to the World Heritage list. In *Metsähallitus Western Finland Natural Heritage Services, West Finland Regional Environment Centre*; Regional Council of Ostrobothnia: Vaasa, Finland, 2004; p. 12.
46. Breilin, O.; Kotilainen, A.; Nenonen, K.; Räsänen, M. The unique moraine morphology, stratotypes and ongoing geological processes at the Kvarken Archipelago on the land uplift area in the western coast of Finland. In *Quaternary Studies in the Northern and Arctic Regions of Finland, Proceedings of the Workshop Organized within the Finnish National Committee for Quaternary Research (INQUA), Kilpisjärvi Biological Station, Finland, 13–14 January 2005*; Ojala, A.E.K., Ed.; Special Paper 40; Geological Survey of Finland: Espoo, Finland, 2005; pp. 97–111.
47. Kotilainen, A.T.; Kaskela, A.M. Comparison of airborne LiDAR and shipboard acoustic data in complex shallow water environments: Filling in the white ribbon zone. *Mar. Geol.* **2017**, *385*, 250–259. [CrossRef]
48. Karukäpp, R.; Raukas, A. Deglaciation History. In *Geology and Mineral Resources of Estonia*; Raukas, A., Teedumäe, A., Eds.; Estonian Academy Publishers: Tallinn, Estonia, 1997; pp. 263–267. ISBN 9985-50-185-3.

49. Talviste, P.; Hang, T.; Kohv, M. Glacial varves at the distal slope of Pandivere-Neva ice-Recessional formations in western Estonia. *Bull. Geol. Soc. Finl.* **2012**, *84*, 7–19. [CrossRef]
50. Glückert, G. The First Salpausselkä at Lohja, southern Finland. *Bull. Geol. Soc. Finl.* **1986**, *58*, 45–55. [CrossRef]
51. Donner, J. The Younger Dryas age of the Salpausselkä moraines in Finland. *Bull. Geol. Soc. Finl.* **2010**, *82*, 69–80. [CrossRef]
52. Uścinowicz, S. Moreny De Geera na Ławicy Slupskiej-nowe dowody na subakwalną deglacjację obszaru południowego Bałtyku. In Proceedings of the XVIII Konferencja Naukowo-Szkoleniowa. Stratigrafia Plejstocenu Polski, Stara Kiszewa, Poland, 5–9 January 2011. (In Polish)
53. Todd, B.J. De Geer moraines on German Bank, southern Scotian Shelf of Atlantic Canada. Geological Society, London, UK. *Memoirs* **2016**, *46*, 259–260. [CrossRef]
54. Bradwell, T.; Stoker, M.S.; Golledge, N.R.; Wilson, C.K.; Merritt, J.W.; Long, D.; Everest, J.D.; Hestvik, O.B.; Stevenson, A.G.; Hubbard, A.L.; et al. The northern sector of the last British Ice Sheet: Maximum extent and demise. *Earth-Sci. Rev.* **2008**, *88*, 207–226. [CrossRef]
55. Amantov, A.V.; Amantova, M.V. Modeling of postglacial development of Lake Ladoga and eastern part of the Gulf of Finland. *Reg. Geol. Metallog.* **2017**, *69*, 5–14. (In Russian)
56. Spiridonov, M.; Ryabchuk, D.; Kotilainen, A.; Vallius, H.; Nesterova, E.; Zhamoida, V. The Quaternary deposits of the Eastern Gulf of Finland. In *Holocene Sedimentary Environment and Sediment Geochemistry of the Eastern Gulf of Finland, Baltic Sea*; Vallius, H., Ed.; Geological Survey of Finland: Espoo, Finland, 2007; pp. 5–18. ISBN 978-951-69-09-953.
57. Amantov, A.V.; Zhamoida, V.A.; Ryabchuk, D.V.; Spiridonov, M.A.; Sapelko, T.V. Geological structure of submarine terraces of the eastern Gulf of Finland and modeling of their development during postglacial time. *Reg. Geol. Metallog.* **2012**, *50*, 5–27. (In Russian)
58. Amantov, A.; Ryabchuk, D.; Fjeldskaar, W.; Zhamoida, V.; Amantova, M. Possible role of Hydroisostasy in Peculiarities of Late Glacial-Postglacial Sedimentation of the Eastern part of the Gulf of Finland and Lake Ladoga. In *EGU General Assembly, Geophysical Research Abstracts*; EGU General Assembly: Vienna, Austria, 2013; Volume 15.
59. Sergeev, A.; Ryabchuk, D.; Gusentsova, T.; Sorokin, P.; Nesterova, E.; Zhamoida, V.; Spiridonov, M.; Kulkova, M.; Glukhov, V. Reconstruction of the paleorelief of the Littorina Sea coastal zone within St. Petersburg based on a study of the archaeological site Okhta 1.59. *Ger. Anz. Romis.-Ger. Kom. Deutsch. Archaologischen Inst.* **2014**, *92*, 33–59.